CrossMark

ORIGINAL PAPER

# Removal of nicotine from indoor air using titania-modified polypropylene fibers: nicotine decomposition by titania-modified polypropylene fibers

M. Cieślak[1] · H. Schmidt[1] · K. Twarowska-Schmidt[2] · I. Kamińska[1]

**Abstract** Textile materials, because of their specific character, can affect the content of volatile pollutants in the indoor air, including the constituents of tobacco smoke (ETS—environmental tobacco smoke). Polypropylene fibers have a particularly high susceptibility for the sorption of nicotine. Textiles made of polypropylene are often used in different rooms or offices. The aim of the research was to give polypropylene fibers the photocatalytic properties by modifying their surface, using titanium dioxide doped with nanoparticles of silver ($TiO_2$/Ag). Modification of polypropylene fibers with $TiO_2$/Ag increases their susceptibility to sorption of nicotine and accelerates its decomposition. A comparison of the decomposition rate constants for the modified and unmodified fibers shows that the decomposition process runs from 1.6 to 2.9 times faster for the modified fibers depending on the nature of modification, the source of the nicotine and the ambient conditions. It was also found that the strength of modified fibers does not change under irradiation.

✉ M. Cieślak
cieslakm@iw.lodz.pl

[1] Scientific Department of Unconventional Technologies and Textiles, Textile Research Institute, 5/15 Brzezinska St., 92-103 Lodz, Poland

[2] Department of Synthetic Fibres, Institute of Biopolymers and Chemical Fibres, 19/27 Maria Skłodowska–Curie St., 90-570 Lodz, Poland

**Keywords** Environmental tobacco smoke · Nicotine · Photocatalytic degradation · Polypropylene fibers · Sorption · Titanium dioxide

## Introduction

Indoor air quality has significant impact on our health and well-being, particularly because nearly 90% of the life of modern man is spent indoors. More and more attention is paid to the problem of "indirect" smoking, i.e., second-hand smoking (SHS), but also third-hand smoking (THS) (WHO 2010; US Department of Health and Human Services 2006; Hu and DesMeules 2007; IARC 2004; State of California EPA 2005; Nebot et al. 2009; Matt et al. 2011; Petrick et al. 2011; Sleiman et al. 2014; Al-sarraf et al. 2015). This problem refers not only to traditional cigarettes, but to e-cigarettes (Flouris et al. 2013; Stillman et al. 2015; Czogała et al. 2014) as well. Furnishing textile materials constitute a significant element in different rooms: residential, office, public buildings or means of transport. Textile materials, because of their specific character, can affect the content of volatile pollutants in the indoor air, including the constituents of tobacco smoke (ETS—environmental tobacco smoke) (Piade et al. 1999; Cieślak 2006; Cieślak and Schmidt 2004; Chien et al. 2011; Cieślak et al. 2014). The susceptibility of sorption of ETS markers in seven types of fibers was tested, and it was found that polypropylene fibers have a particularly high susceptibility for the sorption of nicotine, which is a highly addictive component and the main marker of ETS (Cieślak et al. 2014). The aim of the research was to give polypropylene fibers the properties of accelerated photocatalytic decomposition of nicotine by modifying the fiber surface, using titanium dioxide doped with nanoparticles of

🌀 Springer

1372

Int. J. Environ. Sci. Technol. (2017) 14:1371–1382

silver (TiO$_2$/Ag) as the decomposition activator. Titanium dioxide, particularly due to the dynamic development of nanotechnology, is now used in many processes of photocatalytic decomposition of organic substances (Fujishima et al. 2008; Ochiai et al. 2010, 2014). It is applied, inter alia, onto textile materials in order to induce self-cleaning properties (Zhang et al. 2012; Cieślak et al. 2015; Bozzi et al. 2005; Dastjerdi and Mojtahedi 2013; Tung and Daoud 2011; Radetic 2013; Cieślak et al. 2009; Bourgeois et al. 2012). In our study, the photocatalytic effectiveness of the fibers was evaluated on the basis of sorption and the nicotine decomposition rate under different conditions. We also studied the effect of the photocatalytic modification on the physicochemical properties of the fibers.

## Materials and methods

The following materials were used in the study: polypropylene granules Moplen HP462R, Basell Orlen Polyolefins, Poland, melt flow index MFI = 25 g/10 min, according to ISO 1133 (230 °C/2,16 kg); a spinning preparation Limanol BF 29, Schill + Seilacher GmbH, Germany, ethanol 95%, POCH, Poland; a dispersant polyoxyethylene glycols HO–(CH$_2$–CH$_2$O)$_n$–H, PCC Exol S.A., Poland; micropowder of titanium dioxide doped with 3% of nanosilver, TiO$_2$/Ag, TJTM, China; surfactant Rokafenol N-8, oxyethylated nonylphenol, Brenntag, Poland; Marlboro class A cigarettes (length, 100 mm) containing 11 mg of tar and 0.8 mg of nicotine per cigarette (declared by the manufacturer); nicotine (NCT), 1-methyl-2-(3-pyridyl) pyrrolidine (molecular mass: 162.23, boiling temperature: 243–248 °C, density: 1.010 g/cm$^3$), Fluka 72290, CAS 54-11-5, puriss. p.a. >99.0%).

### Production and modification of fibers

Polypropylene continuous fibers (multifilaments) were made from the granules by a melt method in a two-stage process consisting of a spinning and drawing. The fibers were spun on a laboratory extruder spinning machine at a temperature of 230 °C, through a 17 orifice spinneret, with a throughput rate of 12.1 g/min, at a spinning speed of 500 m/min. The fibers with linear density of 238 dtex were next drawn on a Rieter J6/2 draw winder with a draw ratio of 3.5 on a heated godet at the temperature of 65 °C and unmodified PP fibers with linear density of 67 dtex were obtained. Fibers were modified with TiO$_2$/Ag by two methods.

*Surface modification in the air–titania fluidized bed (PP/A) during spinning process*

The cylindrical fluidizer with a volume of 580 cm$^3$ was placed directly below the spinner head in the zone under the spinneret. The tank was filled up to ¾ of the height of the cylinder with the titania powder, which under the influence of the air flow formed a fluidized bed. The air flow rate was 4 m$^3$/h. The polymer streams flowing from the spinneret passed through the bed in the non-solidified form, and the TiO$_2$/Ag particles were attached to the surface layer of the fiber. The obtained continuous multifilaments with the linear density of 238 dtex were subjected to 3.5 times drawing on the heated godet with the temperature of about 65 °C.

*Surface modification using ethanol dispersion of TiO$_2$/Ag (PP/E)*

The combined three bundles of multifilaments, each with a linear density of 238 dtex, were draw out in a bath with titania–ethanol dispersion (150 g TiO$_2$/Ag/dm$^3$) and between multirollers of a laboratory stand with a draw ratio of 3.5, at a rate of 10 m/min. The dispersion was continuously stirred in a tank and dispensed into the draw bath and additionally mixed in the bath by the rotation disk.

The modified fibers were subjected to the finishing treatment comprising:

- threefold friction (f) in the system of two parallel syntercorund bars with the diameter of 9.5 mm, encircled altogether with 180°,
- washing (w) in an ultrasonic cleaner for 10 min at 30 °C in distilled water with 0.25 g/dm$^3$ of Rokafenol N-8 surfactant, rinsing in distilled water in triplicate and dried in a dark chamber at 25 °C.

### Analysis of TiO$_2$/Ag and the fibers

The microscopic analysis of fiber surface was carried out on a scanning electron microscope JOEL JSM-35C (Joel, Japan) and a scanning electron microscope VEGA 3 (Tescan, Czech Republic) with the EDX INCA Energy X-ray microanalyzer (Oxford Instruments Analytical, UK) and 3D imaging with the Alicona MeX system. The microscopic images of the surface of the unmodified and modified fibers (Fig. 1) were obtained after their sputtering with gold in the JFC-1100 "FINE COAT" sputter (Joel, Japan). Figure 1 also shows a 3D view of fiber surfaces and values of surface topography parameters, such as average height of selected area (Sa), root-mean-square height of selected area (Sq), maximum peak height of selected area (Sp), maximum valley depth of selected area (Sv), maximum height of selected area (Sz), root-mean-square gradient (Sdq), developed interfacial area ratio (Sdr). Figure 2 presents maps of the distribution of Ti elements on the surface of the modified fibers.

**Fig. 1** Scanning electron microscope images of polypropylene (PP) fibers: PP—unmodified fiber, PP/w—unmodified fiber after washing, PP/A—modified air–titania fluidized fiber, PP/A/f—modified air–titania fluidized fiber after friction, PP/A/w—modified air–titania fluidized fiber after washing, PP/E—modified ethanol dispersion fiber, PP/E/f—modified ethanol dispersion fiber after friction, PP/E/w—modified ethanol dispersion fiber after washing, imagination of 2000 × and 4000 × and results of 3D surface analysis; 3D images of fibers surface and topography parameters for PP/w, PP/A, PP/E/w fibers
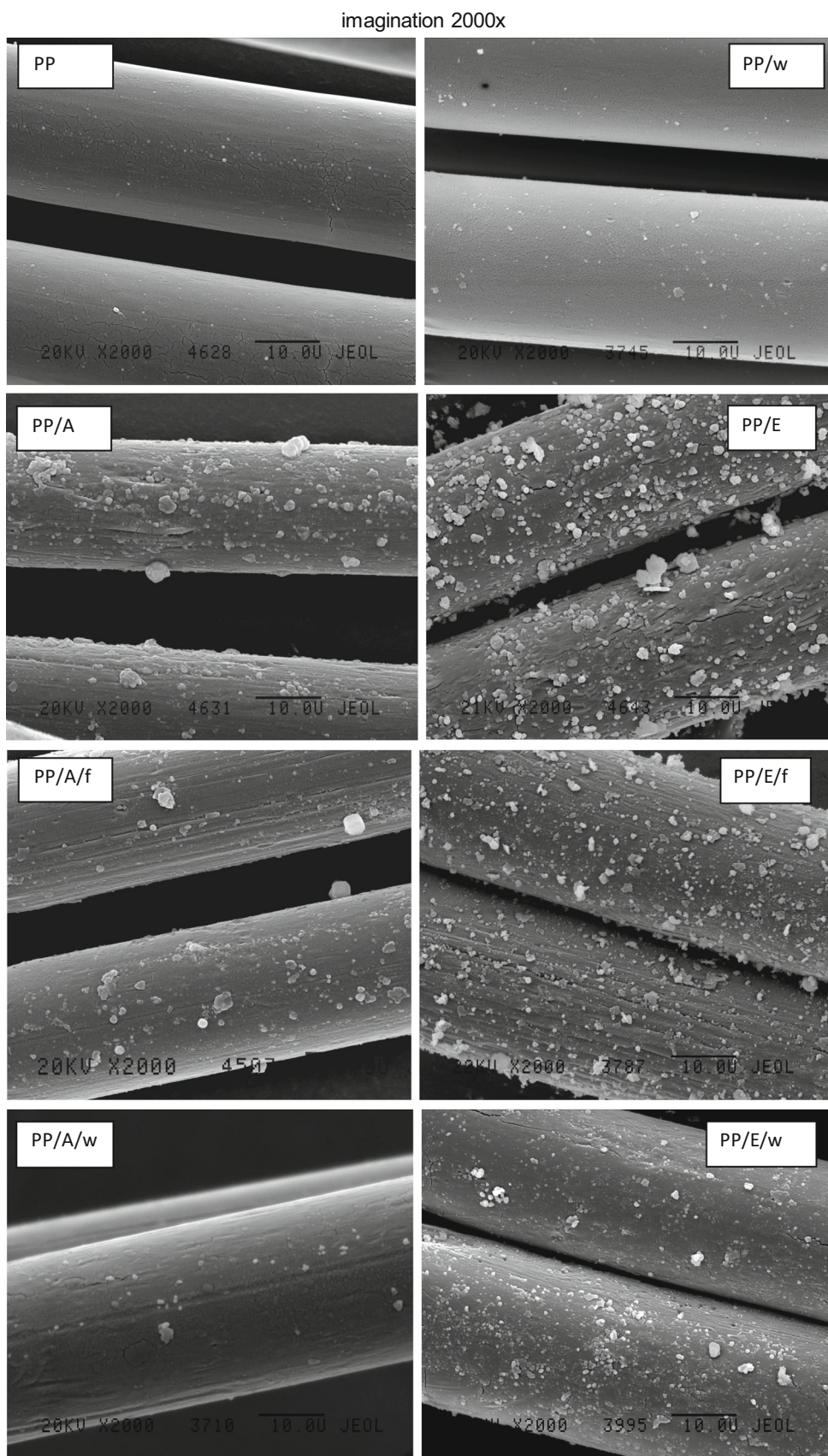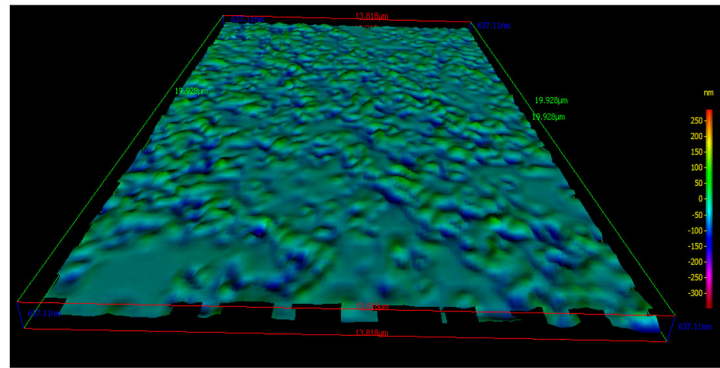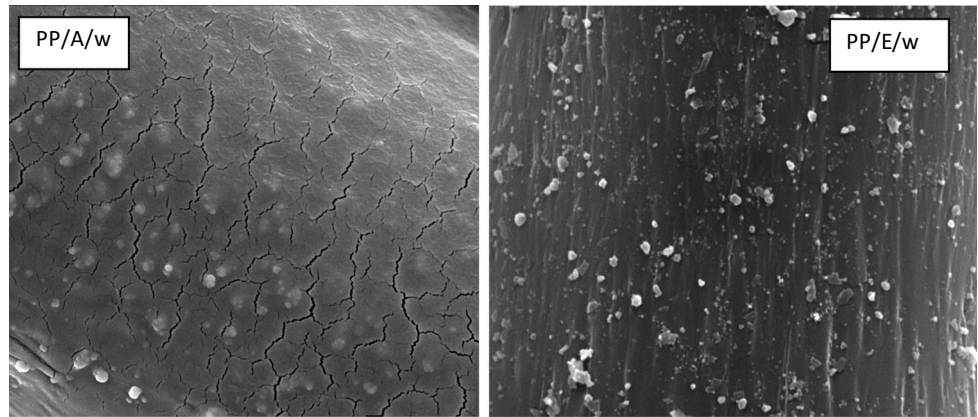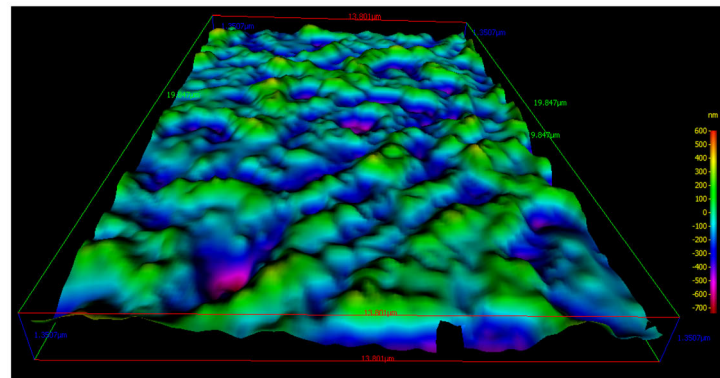
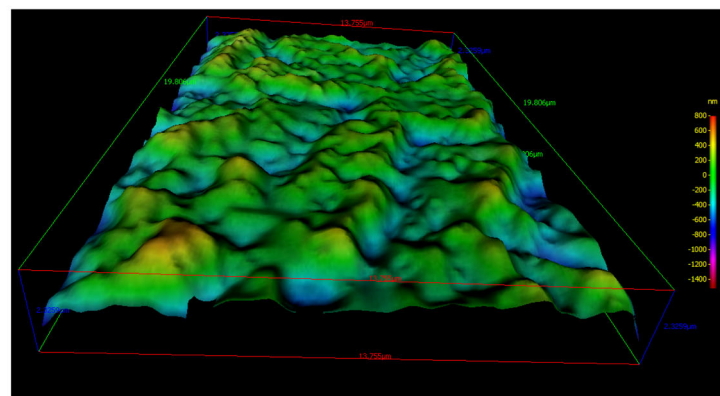imagination 2000x

**Fig. 1** continued

imagination 4000x

PP/w:

Sa 30.40nm

Sq 41.283nm

Sp 283.39nm

Sv 352.6nm

Sz 635.99nm

Sdq 0.54

Sdr 14.64%

PP/A/w:

Sa 69.29nm

Sq 87.579nm

Sp 472.39nm

Sv 410.65nm

Sz 883.04nm

Sdq 0.64

Sdr 19.40%

PP/E/w:

Sa 89.71nm

Sq 113.89nm

Sp 502.94nm

Sv 695.62nm

Sz 1.1986μm

Sdq 0.75

Sdr 27.82%

**Fig. 2** Results of SEM/EDS analysis—distribution of Ti on modified fibers surface (map of 10,000 μm² area: PP/A/w—modified air–titania fluidized fiber after washing, PP/E/w—modified ethanol dispersion fiber after washing
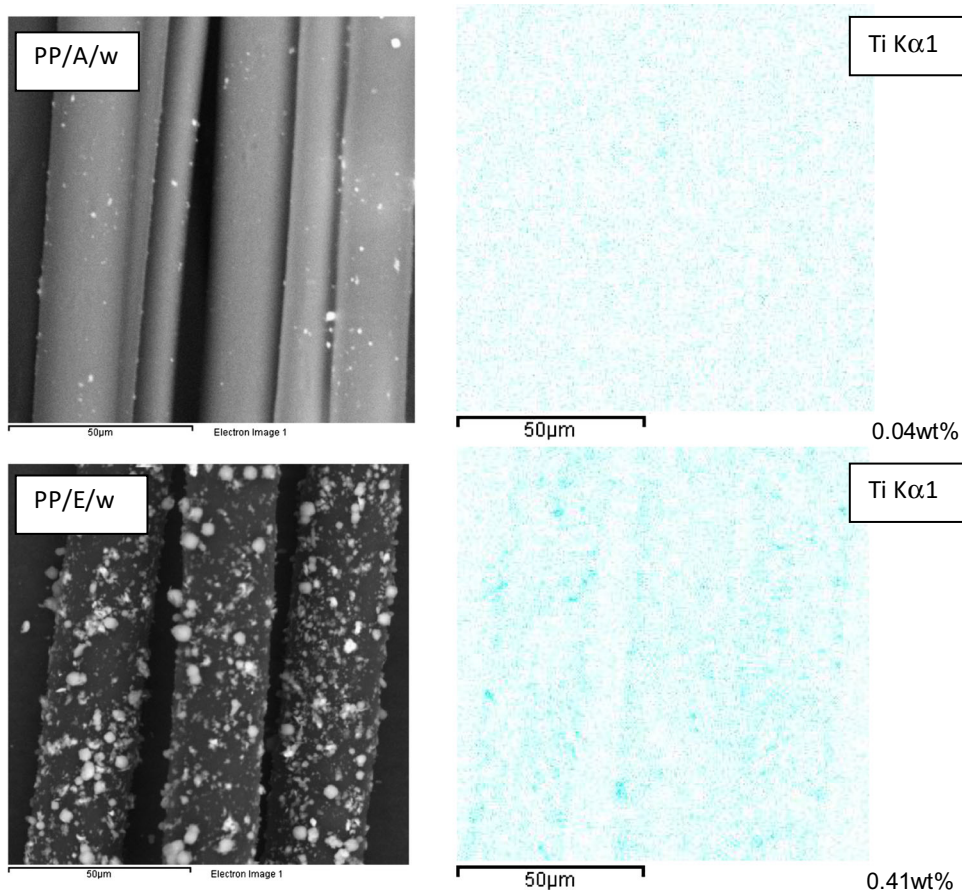


*The specific surface area*

Adsorption isotherms of nitrogen with the purity of 99.998% were determined at −196 °C using the volumetric adsorption analyzer ASAP 2020 (Micromeritics, Norcross, GA, USA) in the range of relative pressures from $10^{-6}$ to 0.995. Before the measurements, all samples were degassed for 2 h at 110 °C. The experimental adsorption isotherms (Fig. 3) were the basis for the calculation of the surface parameters of the tested materials. The BET surface area was determined based on the monolayer capacity using the BET equation (Brunauer–Emmett–Teller) (Brunauer et al. 1938) in the relative pressure range from 0.05 to 0.3. To determine the monolayer capacity, the linear form of the BET equation was used:

$$\frac{\frac{p}{p_o}}{a\left(1 - \frac{p}{p_o}\right)} = \frac{1}{a_m C} \frac{C-1}{a_m C} \frac{p}{p_o} \tag{1}$$

where $a$ is the total absorption in cm³ STP/g, $p/p_o$ is the relative pressure, $a_m$ is the monolayer capacity in cm³ STP/g and $C$ is a constant corresponding to the energy adsorption in the monolayer

$$S_{BET} = a_m \omega N_A \tag{2}$$

where $N_A$ is the Avogadro constant and $\omega$ is the area occupied by a molecule of nitrogen in the monolayer = 0.162 nm².

The values of the monolayer capacity $a_m$, the constant $C$ and the specific surface area $S_{BET}$ determined using Eqs. (1) and (2) are shown in Table 1.

**Sorption experiments**

The fiber samples in the form of bunches were air-conditioned for 24 h at 21 ± 2 °C and 50 ± 5% RH. Sorption experiments were performed in the same conditions on the previously described test stand (Cieślak et al. 2009). Ten samples from each type of fibers (each about 0.05 g) were used in every sorption experiment, and three repetitions were applied. The bunches were hung in a sorption chamber, and after removal of air to the pressure of 20 mmHg, a source of nicotine was supplied into the chamber. In each experiment, 5 μl of NCT or one cigarette was used. NCT in vapor form was directly supplied from a U-shaped tube heated in the glycerol bath. In the case of ETS, the main stream (MS) and the side stream (SS) were supplied from a cigarette smoke device, using the volumetric flow rate of 4 dm³/min. After introducing NCT or ETS, the chamber was closed and left for 24 h. Sorption was carried out with the access to light (l) and in the dark (d),

1376

Int. J. Environ. Sci. Technol. (2017) 14:1371–1382

**Fig. 3** Brunauer–Emmett–Teller adsorption isotherms of nitrogen at −196 °C obtained for: PP—unmodified fiber, PP/w—unmodified fiber after washing, PP/A—modified air–titania fluidized fiber, PP/A/w—modified air–titania fluidized fiber after washing, PP/E—modified ethanol dispersion fiber, PP/E/f—modified ethanol dispersion fiber after friction, PP/E/w—modified ethanol dispersion fiber after washing
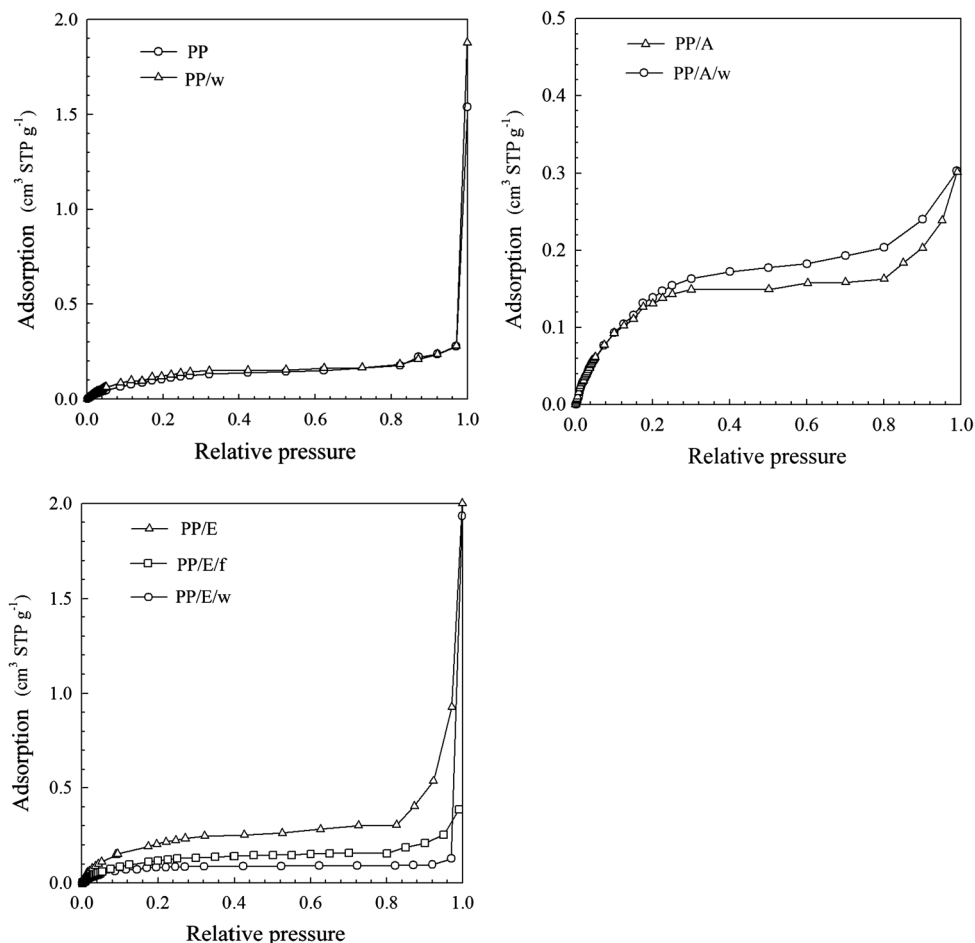


**Table 1** Data determined on the basis of Brunauer–Emmett–Teller adsorption isotherms of nitrogen at −196 °C

| Material | $a_m$, cm$^3$ STP/g | C | $S_{BET}$, m$^2$/g |
|---|---|---|---|
| TiO$_2$/Ag | 4.434 | 140 | 19.3 |
| PP | 0.111 | 13 | 0.48 |
| PP/w | 0.121 | 17 | 0.52 |
| PP/A | 0.131 | 15 | 0.57 |
| PP/A/w | 0.148 | 12 | 0.64 |
| PP/E | 0.191 | 24 | 0.83 |
| PP/E/f | 0.106 | 25 | 0.46 |
| PP/E/w | 0.071 | 41 | 0.31 |

respectively, in the chamber without and with a black-out cover. Then, the samples were removed from the chamber and two of them were immediately closed in vials for chromatographic analysis.

**Decomposition experiments**

The remaining samples were used in decomposition experiments which were performed at 21 ± 2 °C and 50 ± 5% RH in varying conditions—light radiation (r), in

darkness with ventilation of one air exchange per hour (v), in darkness without ventilation (d). Periodically, two samples of each type of fibers were removed from the window (r) or from the same chamber as used in the sorption experiment (v, d) and assayed for the concentration of nicotine in the same way as in the case of the samples analyzed immediately after sorption.

*Irradiation of the fibers after sorption*

Fiber samples were exposed to sunlight on a frame attached to the glass window inside the room (spring, geographical coordinates: N 51°45, 696′, E 019°27, 122′). The value of solar energy was recorded every 30 s, using two sensors (Kipp & Zonen B.V.): CMP 3 in the ultraviolet and visible range, 310–2800 nm, and CUV 4 in the ultraviolet range, 305–385 nm (Fig. 4). The radiation doses, PI (CMP 3) and PII (CUV 4), were calculated using the following formula:

$$P = \frac{3.6t\Sigma W}{n} \tag{3}$$

where $P$ is a radiation dose (PI or PII), kJ/m$^2$; $t$ is time, h; $W$ is radiation energy, W/m$^2$; and $n$ is the number of measurements during light exposure.

**Fig. 4** Example of daily irradiation parameters registration: PI—dose of radiation of visible light and near ultraviolet light, PII—dose of UV radiation, RH—relative air humidity, T—air temperature
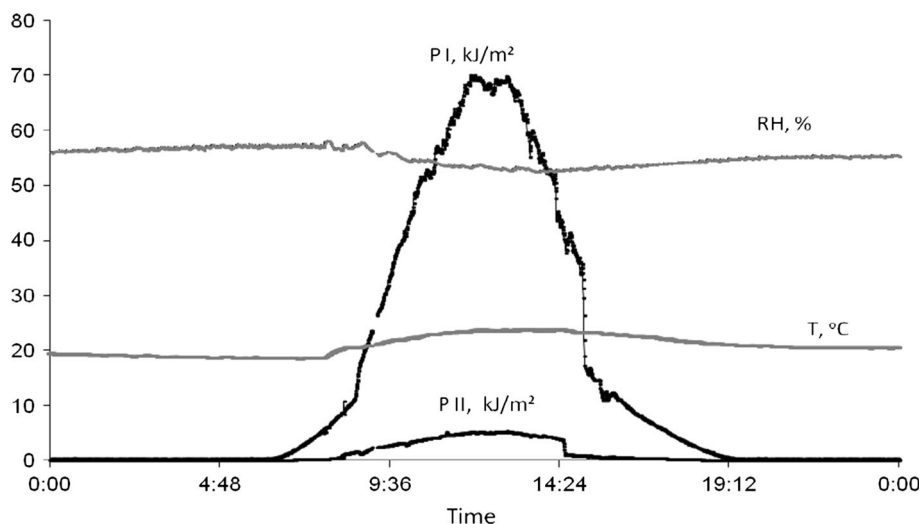


Due to the conditions of the exposition, to assess the impact of the light on the nicotine decomposition the calculated PI radiation doses were used.

### Determination of nicotine concentration and decomposition

The concentration of nicotine in the fibers was determined by gas chromatography technique (Agilent Technologies 6890N). Analysis was performed as described by 16 Cieślak et al. (2014). Figure 5 shows the average nicotine content in the unmodified and modified fibers as determined immediately after CNT sorption performed with the access of light (l) and in the conditions of darkness (d) (-sorption chamber without a black-out cover and with a black-out cover, respectively) and after ETS sorption carried out in the dark (d).

Figure 6 shows relative changes in concentration of nicotine adsorbed from ETS depending on the time of exposure in different conditions.

The decomposition of nicotine adsorbed by the fibers from NCT and ETS was analyzed based on Eq. (4), describing the first-order reaction.

$$c = c_o e^{-kx} \tag{4}$$

where $c$ is the concentration of nicotine determined during the decomposition experiment, μg/g; $c_o$ is the initial concentration of nicotine determined directly after the sorption experiment, μg/g; $x$ is $t$—time, h or PI—radiation dose, kJ/m²; $k$ is the constant rate of nicotine decomposition, /h or m²/kJ, respectively.

Table 2 shows the nicotine decomposition rate constants on the unmodified and modified fibers after NCT sorption performed with the access to light (l) and in the dark (d) and after ETS sorption carried out in the dark (d) based on the time of exposure, determined including and
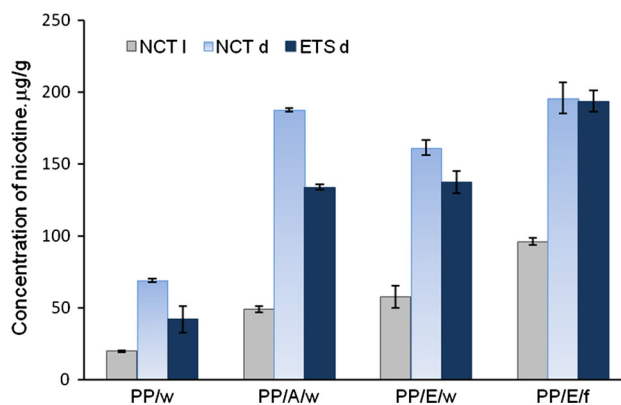


**Fig. 5** Initial concentration of nicotine in fibers after CNT and ETS sorption experiments carried out with the access to light (l) and in the dark (d). PP/w—unmodified fiber after washing, PP/A/w—modified air–titania fluidized fiber after washing, PP/E/f—modified ethanol dispersion fiber after friction, PP/E/w—modified ethanol dispersion fiber after washing

excluding the first hour of the decomposition experiment. Table 3 summarizes the nicotine decomposition rate constants depending on the PI radiation dose.

### Resistance to light

The effect of modifications on the changes in the strength of the fibers under the influence of light was tested in the Xenotest Alpha HE (Atlas, Germany) with an arc xenon lamp with the power of 2200 W, the Xenochrome filter 300 and the outer cylinder made of Suprax glass. The total irradiation dose of 8700 kJ/m² was used. The strength tests were performed on the testing machine Zwick 1120 type CRE (Zwick, Germany). The dependences of the breaking force versus the radiation dose are shown in Fig. 7. The samples of fibers irradiated in the Xenotest were also observed using an electron microscope at the magnification of ×4000.
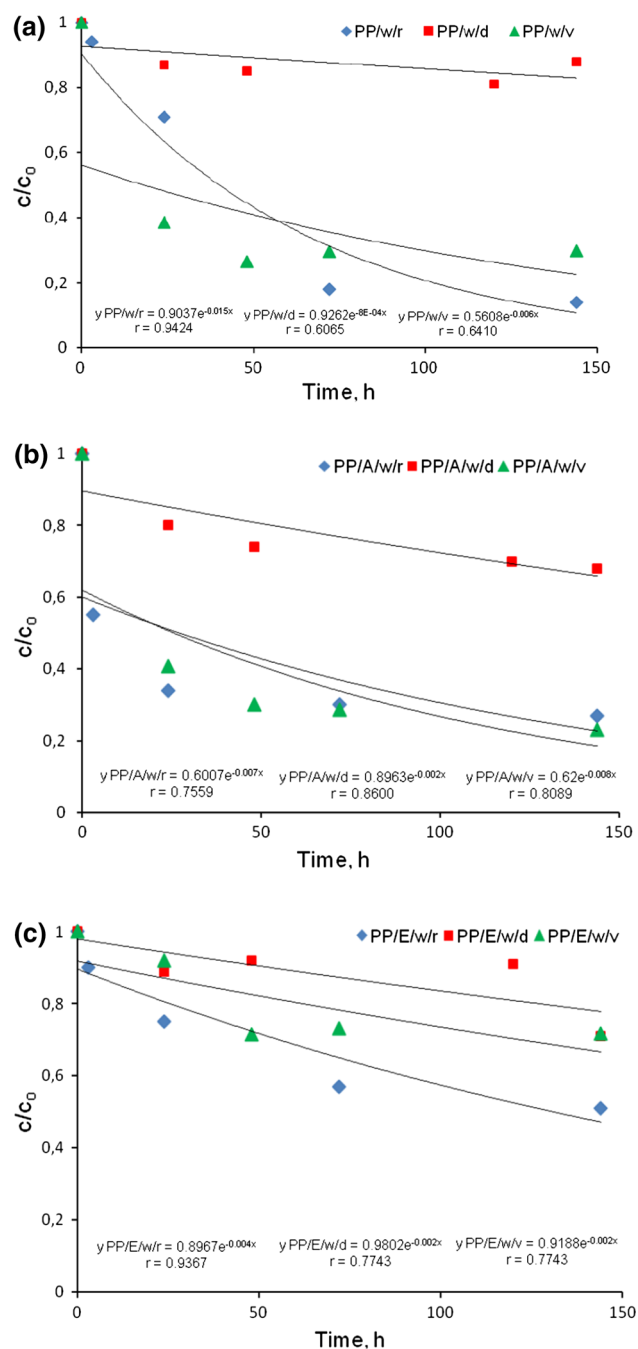
1378

Int. J. Environ. Sci. Technol. (2017) 14:1371–1382



**Fig. 6** Relative changes in the concentration of nicotine in the fibers after ETS sorption depending on the time of exposure in different conditions: light radiation (r), darkness (d), darkness with ventilation (v) for **a** PP/w—unmodified fiber after washing, **b** PP/A/w—modified air–titania fluidized fiber after washing, **c** PP/E/w—modified ethanol dispersion fiber after washing

**Table 2** Nicotine decomposition rate constants depending on the time of the exposure after NCT and ETS sorption with the access to light[a] and in the dark[b]

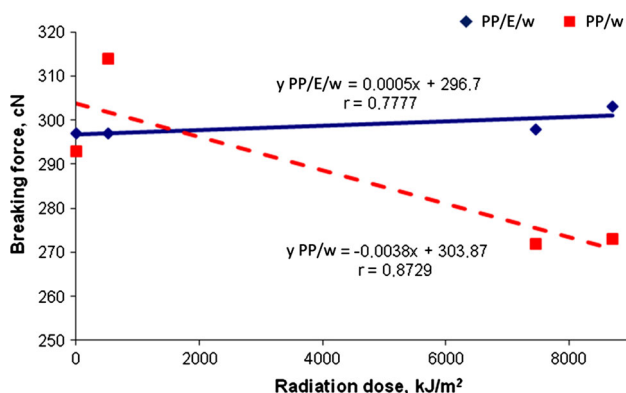| | Unmodified | | Modified | |
|---|---|---|---|---|
| | PP/w | PP/A/w | PP/E/w | PP/E/f |
| *Including the first hour of the exposure* | | | | |
| $k_{NCTl}$, /h | 0.099 | 0.138 | 0.161 | 0.291 |
| $k_{NCTd}$,/h | 0.067 | 0.138 | 0.131 | 0.161 |
| $k_{ETSd}$,/h | 0.098 | 0.207 | 0.164 | 0.178 |
| $NCT_l$ $k_{modified}/k_{unmodified}$ | – | 2.1 | 1.6 | 2.9 |
| $NCT_d$ $k_{modified}/k_{unmodified}$ | – | 2.1 | 2.0 | 2.4 |
| $ETS_d$ $k_{modified}/k_{unmodified}$ | – | 2.1 | 1.7 | 1.8 |
| $r_{NCTl}$ | 0.8802 | 0.8063 | 0.8950 | 0.9414 |
| $r_{NCTd}$ | 0.8867 | 0.9339 | 0.9820 | 0.9547 |
| $r_{ETSd}$ | 0.7564 | 0.9604 | 0.9175 | 0.9648 |
| *Excluding the first hour of the exposure* | | | | |
| $k_{NCTl}$,/h | 0.058 | 0.047 | 0.088 | 0.199 |
| $k_{NCTd}$,/h | 0.041 | 0.099 | 0.112 | 0.123 |
| $k_{ETSd}$,/h | 0.035 | 0.166 | 0.128 | 0.150 |
| $NCT_l$ $k_{modified}/k_{unmodified}$ | – | 0.8 | 1.5 | 3.4 |
| $NCT_d$ $k_{modified}/k_{unmodified}$ | – | 2.4 | 2.7 | 3.0 |
| $ETS_d$ $k_{modified}/k_{unmodified}$ | – | 4.7 | 3.7 | 4.3 |
| $r_{NCTl}$ | 0.8232 | 0.8894 | 0.9919 | 0.9806 |
| $r_{NCTd}$ | 0.9850 | 0.9936 | 0.9999 | 0.9993 |
| $r_{ETSd}$ | 0.9076 | 0.9828 | 0.8871 | 0.9674 |

[a] Sorption chamber without a black-out cover (l)

[b] Sorption chamber with a black-out cover (d)

TiO$_2$/Ag and subsequent processing—friction (f) and washing (w). The fibers differ in surface topography and the method of "incorporation" of titanium dioxide particles and its content (Figs. 1, 2). The final form of the modified fibers in an air–titania fluidized bed after washing (PP/A/w) is characterized by a small number of titanium dioxide particles present on the surface. The dominant are particles embedded in the surface layer of the fiber. The fibers modified with ethanol dispersion have a surface with multiple particles of titanium dioxide (PP/E). The process of friction (PP/E/f) reduces the number of particles loosely fixed to the surface, including these in larger aggregates. After washing (PP/E/w), particles remain that are embedded in the surface, but they are not coated with a polymer, as in the case of fibers modified in the air–titania fluidized bed.

These differences are reflected in the size of the BET specific surface area (Fig. 3; Table 1). The $S_{BET}$ values after washing for the fibers unmodified, modified in the air–titania fluidized bed and in ethanol dispersion are, respectively, 0.52, 0.64 and 0.31 m$^2$/g. Analyzing the values shown in Table 1, it should be noted that the modified and

## Results and discussion

### Structure and morphology

The surfaces of the modified fibers presented by the SEM images (Fig. 1) vary depending on the method of applying

**Table 3** Summary of nicotine decomposition rate constants depending on the PI radiation dose after NCT and ETS sorption with the access to light and in the dark

|  | Unmodified | | Modified | |
|---|---|---|---|---|
|  | PP/w | PP/A/w | PP/E/w | PP/E/f |
| *NCT light* | | | | |
| $k_{NCTl}$, m$^2$/kJ | 0.096 | 0.096 | 0.124 | 0.147 |
| $c_{ol}$, µg/g | 17.449 | 35.341 | 43.767 | 57.066 |
| $k_{modified}/k_{unmodified}$ | – | 1.0 | 1.3 | 1.5 |
| $c_{omodified}/c_{ounmodified}$ | – | 2.0 | 2.5 | 3.3 |
| $r_{NCT}$ | 0.9579 | 0.8786 | 0.9311 | 0.8057 |
| *NCT darkness* | | | | |
| $k_{NCTd}$, m$^2$/kJ | 0.005 | 0.010 | 0.010 | 0.012 |
| $c_{od}$, µg/g | 57.456 | 139.43 | 133.48 | 144.65 |
| $k_{modified}/k_{unmodified}$ | – | 2.0 | 2.0 | 2.4 |
| $c_{omodified}/c_{ounmodified}$ | – | 2.4 | 2.3 | 2.5 |
| $r_{NCTd}$ | 0.7821 | 0.8463 | 0.9296 | 0.8835 |
| *ETS darkness* | | | | |
| $k_{ETSd}$, m$^2$/kJ | 0.006 | 0.013 | 0.010 | 0.011 |
| $c_{od}$, µg/g | 28.946 | 96.374 | 104.21 | 151.4 |
| $k_{modified}/k_{unmodified}$ | – | 2.2 | 1.7 | 1.8 |
| $c_{omodified}/c_{ounmodified}$ | – | 3.3 | 3.6 | 5.2 |
| $r_{ETSd}$ | 0.6512 | 0.9071 | 0.8560 | 0.9141 |



**Fig. 7** Changes of the breaking force for PP/w and PP/E/w fibers after irradiation in the Xenotest

unmodified fibers are nonporous materials with very low surface areas not exceeding 1 m$^2$/g. Comparing the values of *C*, which corresponds to the nitrogen adsorption energy in the monolayer, it can be concluded that the interaction of nitrogen molecules with fibers surfaces is poor. TiO$_2$/Ag material is nonporous, with the possible small proportion of macropores of large dimensions. Specific surface area of TiO$_2$/Ag is not too large, but substantially greater than the specific surface areas of the fibers. Also the value of the constant *C* is much higher and indicates a stronger

interaction of nitrogen molecules with the surface of titania materials. The fibers under the study are the nonporous materials with a small surface area, hence the small adsorption properties of nitrogen. We also found no correlation between the values of BET surface area and susceptibility of fibers to sorption of nicotine. Therefore, we discuss the results based on the other mechanism that affect the sorption of nicotine.

## Mechanism of sorption and decomposition of nicotine

Sorption and decomposition of nicotine on the fibers are affected by the physicochemical characteristics of the sorbate and the textile and non-textile sorbents (Cieślak et al. 2014; Cooks 1999; Banyasz 1999; Gregg and Sing 1967; Adamson and Gast 1997), and they also depend on the ambient conditions under which these processes occur (Weschler and Nazaroff 2008). Nicotine is a bicyclic alkaloid characterized by amphiphilic properties, because its molecule possesses both a hydrophilic and a hydrophobic part. Nitrogen atoms of pyridine and pyrrolidine cycles allow hydrogen bond with water, while hydrocarbon rest of the molecule is hydrophobic. Nicotine is miscible in water and soluble in alcohol, chloroform, ether, petroleum ether and oils, but its actual solution behavior is dependent by ambient condition. Nicotine is a semi-volatile component of ETS present in both gaseous and partial fractions (IARC 2004).

PP fibers are known for extremely hydrophobic properties. Due to a low value of molecular cohesion energy, the water binding is impossible (Van Krevelen 1990). The amount of water absorbed from atmosphere with 65% RH at 21 °C is 0.03–0.05%. The Hansen solubility parameters for nicotine, polypropylene and water are 21.10, 18.8 and 23.4 J$^{1/2}$/cm$^{3/2}$, respectively (Hansen 2007). The differences in the values of solubility parameters for nicotine/polypropylene and water/polypropylene amounted to 2.3 and 6.6, J$^{1/2}$/cm$^{3/2}$, respectively. The nearly three times greater difference between solubility parameters favors nicotine in polymer solvent affinity. On the other hand, the difference between nicotine and water solubility parameters is also 2.3 J$^{1/2}$/cm$^{3/2}$. In the Pat. US4736755 (1988) described that polypropylene polymer is an efficient nicotine adsorbent at 25 °C and the loss of nicotine after 10 min vacuum desorption is negligible. Therefore, cumulated nicotine can remain in polypropylene fibers for a long time, especially when the access to light and oxygen is limited.

The presence of titania particles can also changed the moisture conditions of fiber surface and susceptibility to nicotine sorption and decomposition. The air relative humidity of the sample conditioning and sorption

1380

Int. J. Environ. Sci. Technol. (2017) 14:1371–1382

experiment was 50 ± 5%. Such humidity does not change the moisture of polypropylene, but influences the moisture of the titania modifier. The powder of titanium dioxide adsorbs water from the atmosphere. Water vapor interacts with titania dioxide, and surface hydroxyls can affect adsorption and reaction processes (Henderson 2002). Most authors agree that water is firstly adsorbed in a dissociative manner and then the formed surface hydroxyls allow physisorption of further molecules by hydrogen bonding (Henderson 2002; Nosaka et al. 2004). In the practical conditions, titania photocatalysts work in the presence of physisorbed water. Nosaka et al. (2004) conclude that photocatalytical oxidation of organic pollutants can be favored in the physisorbed water layer rather than on the solid surface.

The differences in the physicochemical structure of the fibers influence the effects of nicotine sorption and decomposition. For the unmodified PP fibers, in the case of NCT sorption, direct diffusion is observed into the surface layer of polypropylene. In the case of ETS sorption, the fibers adsorb nicotine from the ETS aerosol and the tar substances deposited on the surface. The PP fibers modified with $TiO_2$/Ag adsorb nicotine from the air both on the fiber surface and on the surface of the $TiO_2$/Ag particles. Nicotine diffuses at different rates into the structure of titanium dioxide and into the polymer. In the absence of light during the sorption, in equilibrium with the concentration of nicotine vapor in the air, the division of nicotine occurs between the fiber polymer and the $TiO_2$/Ag particles. With the availability of light, there occur competitive processes—simultaneous sorption of nicotine and its decomposition on the fiber surface. This is indicated by the initial concentration in the fibers subjected to sorption with or without light (Fig. 5). The decomposition of nicotine under the influence of light is the first-order reaction. Thanks to light and oxygen from the air, nicotine contained in $TiO_2$/Ag undergoes relatively fast decomposition. Nicotine contained in the fiber polymer diffuses into the surface and after adsorption by $TiO_2$/Ag undergoes accelerated decomposition. The decomposition rate is determined inter alia by the rate of nicotine diffusion in the polymer. Based on the rapid decomposition of the nicotine present on the fiber surface (catalyzed by $TiO_2$/Ag), it may be assumed that at the initial stage, decomposition depends proportionally to time, and then, the description of desorption corresponds to an exponential equation. It is indicated by comparing the values of correlation coefficients $r$, determined from Eq. (4) taking into account and excluding the first hour of exposure (Table 2). For the modified fibers, they increase when the first hour of exposure is excluded. This mechanism occurs in the presence of light and oxygen during irradiation of the samples after sorption. A comparison of the rate constants shows that the decomposition

process runs from 1.6 to 2.9 times faster for the modified fibers depending on the nature of modification, the source of the nicotine and the desorption conditions (Table 2). After NCT sorption performed with direct light (l) the fastest decomposition of nicotine was observed for PP/E/f, $k_{modified}/k_{unmodified} = 2.9$. This is due to the fact that after the friction treatment (f) and before washing (w) its surface contains the highest amount of $TiO_2$/Ag (Fig. 1). Washing (PP/E/w) diminishes this amount, and the ratio is reduced to 1.6. Similar relationships exist for PP/E/f and PP/E/w excluding the first hour of exposure, 3.4 and 1.5, respectively. After NCT sorption carried out in the dark (d), the amount of nicotine is diminished the fastest on the PP/E/f fiber, but the decomposition rate constants for the modified fibers are more similar to one another. In the case of ETS sorption in the dark, the fastest nicotine decline occurs for the fibers modified in an air–titania fluidized bed PP/A/w (Table 2; Fig. 6). The decline of nicotine in unmodified fibers is twice more slowly.

Comparing the decomposition rates of nicotine depending on the PI radiation dose (Table 3), it was found that the fastest rate referred to the fibers which adsorbed NCT under light conditions, and the highest value of the desorption constant was noted for PP/E/f and equaled 0.147 $m^2$/kJ, and the lowest was observed for the unmodified PP/w and the one modified in the air–titania fluidized bed, 0.096 $m^2$/kJ. The constants determined for the fibers which adsorbed nicotine from NCT and ETS in the dark are lower by more than an order of magnitude. It is characteristic that the level of nicotine decreases is over 19 times slower for the unmodified fiber after NCT sorption in the dark, than for the sorption experiment with the access to light. In the case of modified fibers, the ratio of the rate constants is 9.6, 12.4 and 12.3, respectively, for PP/A/w, PP/E/w and PP/E/f.

The studies of the influence of ambient conditions on the relative loss of nicotine adsorbed from ETS (Fig. 6) show that the slowest reduction occurs for the fiber in the dark without the exchange of air and oxygen availability (d), the decomposition rate constants for PP/w, PP/A/w and PP/E/w are, respectively, 0.0008, 0.002 and 0.002/h. Under the conditions of darkness and ventilation (v), the values of these constants increase for PP/w and PP/A/w and equal, respectively, 0.006 and 0.008/h. For the PP/E/w sample, the value remains unchanged. Under the influence of light exposure, the $k$ values increase for all the samples and equal 0.015, 0.007 and 0.004/h, respectively.

The presence of titanium dioxide on the fibers increased nicotine sorption and hastened its decomposition. Similar results were obtained for modified cellulose fibers (Giesz et al. 2016).

The rate of nicotine decomposition is determined by the nature of fibers modification and the access of light and

oxygen. The treatment of friction and subsequent washing admittedly reduces the photocatalytic efficiency of the modified fibers by removing the modifier unconnected with the fiber. Such design of products modified with nanoparticles, however, is in line with the strategy of reducing the risk of releasing the modifier nanoparticles into the environment (Wąsowicz et al. 2011; Roszak et al. 2013).

### Resistance to light

Functionalization of the fibers should give them added value without compromising the basic properties, including a durability. It was found that the strength of modified fibers does not change under irradiation. There was no damage to the fiber surface in the form of transverse cracks characteristic of the photo-oxidative degradation of PP fibers (Barish 1989). The strength of unmodified fibers is reduced (Fig. 7), and small longitudinal cracks are formed on their surface when they are exposed to the light. $TiO_2$/Ag protects the fibers against absorption of a part of UV light and degradation of polypropylene.

### Conclusions

Modification of polypropylene fibers with $TiO_2$/Ag increases their susceptibility to sorption of nicotine in gaseous form, both from NCT and ETS, and accelerates decomposition compared to the unmodified fibers. In rooms contaminated with ETS, interior textiles made from PP fibers modified with $TiO_2$/Ag can thus affect the reduction of nicotine concentration in the air and reduce a risk of involuntary inhalation of nicotine, highly addictive component of ETS.

### References

Adamson AW, Gast AP (1997) Adsorption of gases and vapors on solids. In: Physical chemistry of surfaces, 6th edn. Wiley-Interscience, New York, pp 599–676

Al-sarraf AA, Yassin MF, BouhamraInt W (2015) Experimental and computational study of particulate matter of secondhand smoke in indoor environment. J Environ Sci Technol 12:73–86

Banyasz JL (1999) The physical chemistry of nicotine. In: Gorrod JW, Jacob PIII (eds) Analytical determination of nicotine and related compounds and their metabolites. Elsevier, Amsterdam, pp 149–190

Barish L (1989) Sunlight degradation of polypropylene textile fibres: a microscopical study. J Text Inst 80:107–119

Bourgeois PA, Puzenata E, Peruchon L, Simonet F, Chevalier D, Deflin E, Brochier C, Guillard Ch (2012) Characterization of a new photocatalytic textile for formaldehyde removal from indoor air. Appl Catal B-Environ 128:171–178

Bozzi A, Yuranova T, Guasaquillo I, Laub D, Kiwi J (2005) Self-cleaning of modified cotton textiles by $TiO_2$ at low temperatures under daylight irradiation. J Photochem Photobiol, A 174:156–164

Brunauer S, Emmett PH, Teller E (1938) Adsorption of gases in multimolecular layers. J Am Chem Soc 60:309–319

Chien YC, Chang CP, Liu ZZ (2011) Volatile organics off gassed among tobacco-exposed clothing fabrics. J Hazard Mater 193:139–148

Cieślak M (2006) New approach to environmental tobacco smoke exposure and its relation to reemission processes. Int J Occup Med Environ 19:92–98

Cieślak M, Schmidt H (2004) Contamination of wool fibre exposed to environmental tobacco smoke. Fibres Text East Eur 12:81–83

Cieślak M, Schmidt H, Świercz R, Wąsowicz W (2009) $TiO_2$/Ag modified carpet fibres for reduction of nicotine exposure. Fibres Text East Eur 17:59–65

Cieślak M, Schmidt H, Świercz R, Wąsowicz W (2014) Fibers susceptibility to contamination by environmental tobacco smoke markers. Text Res J 84:840–853

Cieślak M, Celichowski G, Giesz P, Nejman A, Puchowicz D, Grobelny J (2015) Formation of nanostructured $TiO_2$-anatase films on the basalt fiber surface. Surf Coat Technol 276:686–695

Cooks PA (1999) Chemical properties of nicotine and other tobacco-related compounds. In: Gorrod JW, Jacob P III (eds) Analytical determination of nicotine and related compounds and their metabolites. Elsevier, Amsterdam, pp 69–147

Czogała J, Goniewicz ML, Fidelus B, Zielinska-Danch W, Travers MJ, Sobczak A (2014) Secondhand exposure to vapors from electronic cigarettes. Nicot Tob Res 16:655–662

Dastjerdi R, Mojtahedi MRM (2013) Multifunctional melt-mixed Ag/$TiO_2$ nanocomposite PP fabrics: water vapour permeability, UV resistance, UV protection and wear properties. Fiber Polym 14:298–303

Flouris AD, Chorti MS, Poulianiti KP, Jamurtas AZ, Kostikas K, Tzatzarakis MN, Hayes AW, Tsatsakis AM, Koutedakis Y (2013) Acute impact of active and passive electronic cigarette smoking on serum cotinine and lung function. Inhal Toxicol 25:91–101

Fujishima A, Zhang X, Tryk DA (2008) $TiO_2$ photocatalysis and related surface phenomena. Surf Sci Rep 63:515–582

Giesz P, Celichowski G, Puchowicz D, Kamińska I, Grobelny J, Batory D, Cieślak M (2016) Microwave-assisted $TiO_2$: anatase formation on cotton and viscose fabric surfaces. Cellulose 23:2143–2159

Gregg SJ, Sing KSW (1967) Adsorption surface area and porosity. Academic Press, London

Hansen CM (2007) Hansen solubility parameters. A user's handbook, 2nd edn. CRC Press, Boca Raton

Henderson MA (2002) The interaction of water with solid surfaces: fundamental aspects revisited. Surf Sci Rep 46:1–308

Hu J, DesMeules M (2007) Environmental tobacco smoke and cancer. In: Jeorgensen NA (ed) Passive smoking and health research. Nova Science Publishers, Inc., New York, pp 215–243

1382

Int. J. Environ. Sci. Technol. (2017) 14:1371–1382

IARC (2004) Monographs on the evaluation of carcinogenic risks to humans. Tobacco smoke and involuntary smoking. IARC Press, Lyon

Matt GE, Quintana PJE, Destaillats H, Gundel LA, Sleiman M, Singer BC, Jacob PIII, Benowitz N, Winickoff JP, Rehan V, Talbot P, Schick S, Samet J, Wang Y, Hang B, Martins-Green M, Pankow JF, Hovell MF (2011) Thirdhand tobacco smoke. Emerging evidence and arguments for a multidisciplinary research agenda. Environ Health Perspect 119:1218–1226

Nebot M, Lopez MJ, Ariza C, Perez-Rios M, Fu M, Schiaffino A, Munoz G, Salto E, Fernandez E (2009) Impact of the Spanish smoking law on exposure to secondhand smoke in offices and hospitality venues. Before-and-after study. Environ Health Perspect 117:344–347

Nosaka AY, Fujiwara T, Yagi H, Akutsu H, Nosaka Y (2004) Characteristics of water adsorbed on $TiO_2$ photocatalytic systems with increasing temperature as studied by solid-state $^1$H NMR spectroscopy. J Phys Chem B 108:9121–9125

Ochiai T, Fukuda T, Nakata K, Murakami T, Tryk DA, Koide Y, Fujishima A (2010) Photocatalytic inactivation and removal of algae with $TiO_2$-coated materials. J Appl Electrochem 40:1737–1742

Ochiai T, Ichihashi E, Nishida N, Machida T, Uchida Y, Hayashi Y, Morito Y, Fujishima A (2014) Field performance test of an air-cleaner with photocatalysis-plasma synergistic reactors for practical and long-term use. Molecules 19:17424–17434

Pat. US4736755 (1988)

Petrick LM, Svidovsky A, Dubowski Y (2011) Thirdhand Smoke: heterogeneous oxidation of nicotine and secondary aerosol formation in the indoor environment. Environ Sci Technol 45:328–333

Piade JJ, D'Andres S, Sanders EB (1999) Sorption phenomena of nicotine and ethenylpyridine vapors on different materials in a test chamber. Environ Sci Technol 33:2046–2052

Radetic M (2013) Functionalization of textile materials with $TiO_2$ nanoparticles. J Photochem Photobiol, C 16:62–76

Roszak J, Stępnik M, Nocuń M, Ferlińska M, Smok-Pieniążek A, Grobelny J, Wąsowicz W, Cieślak M (2013) A strategy for in vitro safety testing of nanotitania-modified textile products. J Hazard Mater 256–257:67–75

Sleiman M, Logue JM, Luo W, Pankow JF, Gundel LA, Destaillats H (2014) Inhalable constituents of thirdhand tobacco smoke: chemical characterization and health impact considerations. Environ Sci Technol 48:13093–13101

State of California Environmental Protection Agency (2005) Air resources board: proposed identification of environmental tobacco smoke as a toxic air contaminant, appendix III, part B, p ES-4. http://www.arb.ca.gov/regact/ets2006/app3partb.pdf

Stillman FA, Soong AL, Zheng Y, Navas-Acien A (2015) E-cigarette use in air transit: self-reported data from US flight attendants. Tob Control 24:417–418

Tung WS, Daoud WA (2011) Self-cleaning fibers via nanotechnology: a virtual reality. J Mater Chem 21:7858–7869

US Department of Health and Human Services (2006) The health consequences of involuntary exposure to tobacco smoke: a report of the surgeon general Public Health Service, Office of the Surgeon General, Rockville, MD. http://www.surgeongeneral.gov/library/secondhandsmoke/report/

Van Krevelen DW (1990) Cohesive properties and solubility. Properties of polymers, 3rd edn. Elsevier, Amsterdam, pp 189–224

Wąsowicz W, Cieślak M, Palus J, Stańczyk M, Dziubałtowska M, Stępnik M, Düchler M (2011) Evaluation of biological effects of nanomaterials. Part I. Cyto- and genotoxicity of nano-silver composites applied in textile technologies. Int J Occup Environ Health 24:348–358

Weschler CJ, Nazaroff WW (2008) Semivolatile organic compounds in indoor environments. Atmos Environ 42:9018–9040

WHO guidelines for indoor air quality: selected pollutants (2010) The WHO European Centre for Environment and Health, Bonn Office, WHO Regional Office for Europe coordinated the development of these WHO guidelines

Zhang H, Zhu H, Sun R (2012) Fabrication of photocatalytic $TiO_2$ nanoparticle film on PET fabric by hydrothermal method. Text Res J 82:747–754